

# Measurement of the performance of the ATLAS RPC detector in 2015 LHC pp run at $\sqrt{s} = 13$ TeV

G. Chiodini <sup>a</sup>, S. Spagnolo <sup>a,b</sup> for the ATLAS RPC Group.

<sup>a</sup>Istituto Nazionale di Fisica Nucleare sez. di Lecce, Italy.

<sup>b</sup>Dipartimento di Matematica e Fisica "Ennio De Giorgi", Università del Salento, Italy.

The RPC detector has been running steadily during the ATLAS data taking of 2015. The detailed performance in terms of detector efficiency and muon trigger efficiency has been measured with a large data set recorded during the LHC pp run with 25 ns spacing between colliding bunches at  $\sqrt{s} = 13$  TeV. While these data, corresponding to an integrated luminosity of  $2.3 \text{ fb}^{-1}$ , were collected the RPC system was running in rather stable conditions. Therefore, the sample allows a careful study of the response of the system and, in addition, the strip-panel efficiencies and cluster size distributions measured with it are a valuable input for the production of a new round of the official ATLAS simulation production. These MC samples are currently being processed and will reproduce with good accuracy the running conditions for each detector as observed in the most recent data taking, thanks to the emulation, at digitisation level, of the measured detector conditions. The  $\eta \times \phi$  distribution of the RPC hits in the pivot plane contributing to high  $p_T$  muon triggers in the barrel of ATLAS is shown in fig. 1. The grid of the strip panels, showing the segmentation of the RPC detector in the pivotal plane of the trigger logic, is superimposed to the distribution of the trigger hits. The un-instrumented region around  $\eta = 0$  correspond to holes in the barrel structure dictated by services; the holes in the acceptance at around  $\phi = -1$  and  $\phi = -2$  correspond to the region of the ATLAS feet, where the mechanical structures supporting the ATLAS calorimeters prevent an hermetic coverage of the barrel. BME and BOE RPC chambers, as well as the extra BOG and BOF chambers in the outer part of the feet sectors are not shown in this plot, since the commissioning of most of these chambers and the integration in the ATLAS DAQ didn't take place until the end of the 2015 run.

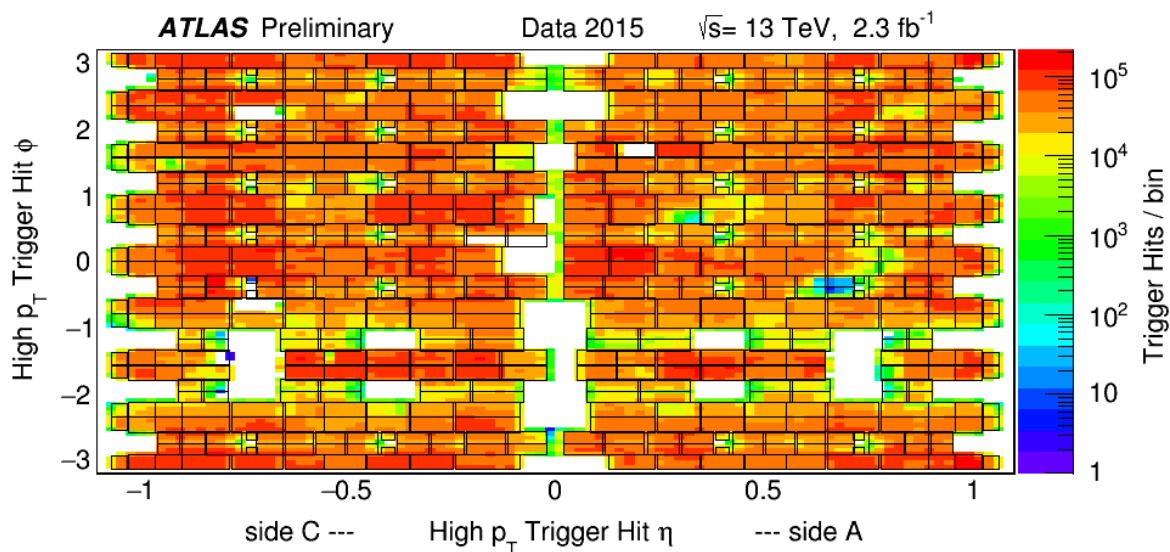


Figure 1. Distribution of the RPC trigger hits in the pivot layer associated with a high- $p_T$  trigger. The  $\phi$  and  $\eta$  coordinates of the strips producing the trigger are used to locate the hit in the  $\eta \times \phi$  plane. The black lines indicate the contours of individual RPC strip panels. The data set corresponds to pp collisions collected with 25 ns spacing between colliding bunches.

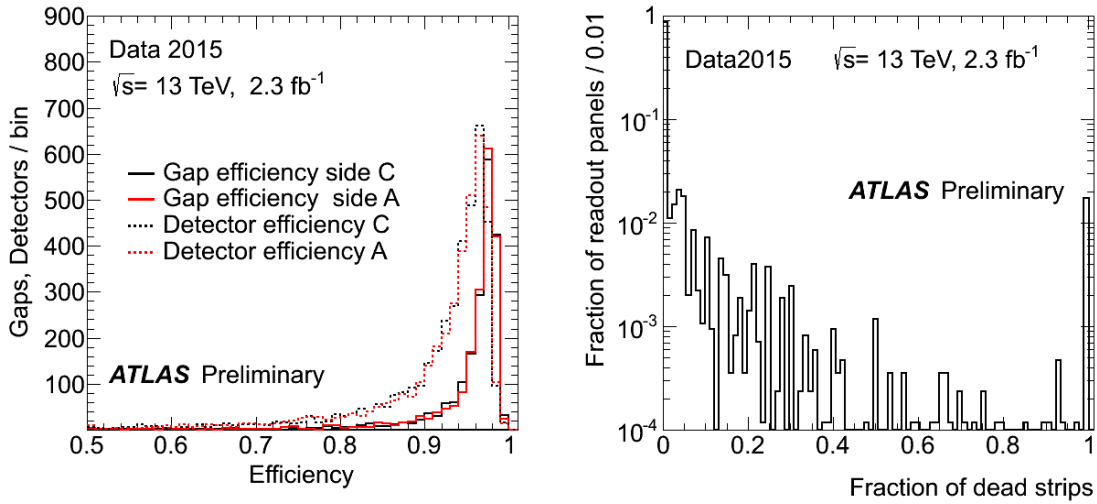


Figure 2. Left plot: Distribution of the measured RPC "gap efficiency" of each gas volume, defined by the presence of hits on at least one of the two strip panels ( $\eta$  and  $\phi$ ), and of the "detector efficiency" for each strip panel, defined by the presence of hits in the strip panel. The total number of panels ( $\eta + \phi$ ) is 8592, the number of gaps is 4296. Right plot: Distribution of the fraction of dead strips per readout panel for both views. Dead strips can originate from different reasons, e.g. readout problems, masking of noisy channels or gas gaps disconnected from HV. The peak at 1 shows that the fraction of readout panels in which all strips are dead is approximately 2%.

Most of the measurements reported here are performed with an extended version of the software used for the Offline Data Quality Monitoring of the RPC detector, which runs in the standard reconstruction chain and provided input to the WEB display running for Data Quality shifters and accessible through the WEB with a very short delay during data taking and later. The efficiency is measured using RPC tracks built with RPC hits only, and removing the hits on the unit under test. The entire Physics\_main data-stream is used for the measurement. In fig. 2 the distribution of the efficiency measured for each strip panel and for each gas gap of the RPC system is shown on the left plot. Since each gas gap is readout by a  $\phi$  strip panel on one side and a  $\eta$  strip panel on the other side, the gap efficiency is defined as the efficiency for having signals in at least one of the views and it's clearly slightly higher than the efficiency for having a signal in a given strip panel. The long queue of the distributions is due to localised inefficiency, like dead strips, dead front-end chips (reading sets of 8 strips), harder discrimination thresholds of the front-end electronics. The plot on the right of fig. 2 shows the distribution of the fraction of dead strips in a strip panel. The distribution of the measured efficiencies across the detector is shown (for the  $\phi$  and  $\eta$  strip panels of the two gas gaps in each chamber of the pivot plane) in fig. 3 on the left. In the right plot the efficiency distribution that is being used in input for the current MC production (MC15c) is shown. The difference between the efficiency map as measured and as simulated arise from two factors: strip panels where the efficiency is measured in data with a low statistical precision (less than 100 tracks extrapolated to the panel) are assigned a nominal efficiency corresponding to the peak efficiency measured in 2012 data; strip panels dead or with a measured efficiency lower than 50% are assigned in simulation an efficiency of 50% (this allows to have a simulation always better than the real detector, even in the occurrence of hardware interventions in the winter shutdown that can recover dead detector elements).

The RPC detector efficiency and the finite acceptance of the RPC layout in ATLAS are driving the LVL1 muon trigger efficiency in ATLAS. Fig. 4 (left plot) shows the total (acceptance  $\times$  efficiency) measured LVL1 trigger efficiency at plateau for the trigger thresholds for muons with  $|\eta| < 1.05$  and  $p_T > 15$  GeV both for the low  $p_T$  and a high  $p_T$  trigger topologies. In the plot on the right of 4 the LVL1 efficiency measured in data as a function of  $\phi$  is compared with the prediction of a simulation where the measured detector efficiency (as in fig.2) are emulated with the granularity of the strip panels.

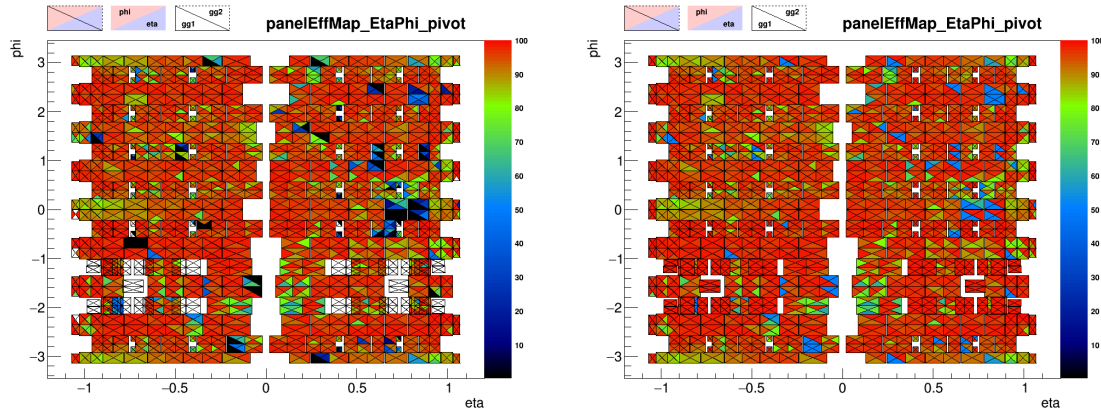


Figure 3. Color-coded map of strip-panel efficiency ( $\phi$  and  $\eta$ ) for the two gas gaps of all RPC in the pivot plane, as measured in 2015 data (25ns bunch crossing sample) -on the left- and as injected in the simulation production to be used in 2016 (conventionally referred as MC15c) -on the right. White area on the left plot correspond to the BME RPC chambers, the extra BOG and BOF in the outer part of the feet sectors and any other strip panel where the measurement was not possible due to lack of extrapolated muon tracks.

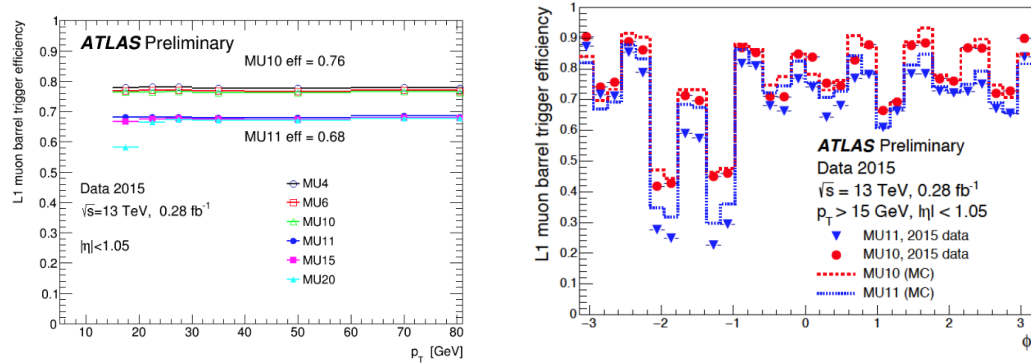


Figure 4. LVL1 muon barrel trigger efficiency for reconstructed muons with  $p_T > 15$  GeV and  $|\eta| < 1.05$  as a function of transverse momentum (left) and  $\phi$  (right). The efficiency is shown for the six Level-1 thresholds: MU4, MU6, MU10 which require a coincidence of the two inner RPC stations, and MU11, MU15, MU20 with a further coincidence on the outer RPC stations. On the right, only one low  $p_T$  and one high  $p_T$  thresholds are shown. The dashed histograms show the results from a special MC simulation which includes measured efficiencies of the RPC chambers. The efficiency was measured using events selected by independent triggers.

## REFERENCES

1. G. Chiodini, M. Corradi, S. Rosati, G. Salamanna, S. Spagnolo, "Plots on RPC / L1 Muon Barrel Trigger Performance in 2015", ATL-COM-MUON-2016-005, <https://cds.cern.ch/record/2131167/>